Ecotoxicology and Environmental Safety 215 (2021) 112093

Contents lists available at ScienceDirect

Ecotoxicology and Environmental Safety

journal homepage: www.elsevier.com/locate/ecoenv

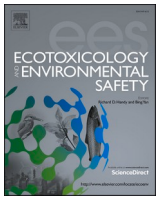

Investigations on inhibitory effects of nickel and cobalt salts on the decolorization of textile dyes by the white rot fungus *Phanerochaete velutina*

Christian Zafiu [a], Florian Part [a,b,*], Eva-Kathrin Ehmoser [b], Mika A. Kähkönen [c]

[a] University of Natural Resources and Life Sciences, Vienna, Department of Water-Atmosphere-Environment, Institute of Waste Management, Muthgasse 107, 1190 Vienna, Austria
[b] University of Natural Resources and Life Sciences, Vienna, Department of Nanobiotechnology, Institute for Synthetic Bioarchitectures, Muthgasse 11, 1190 Vienna, Austria
[c] Department of Microbiology, Faculty of Agriculture and Forestry, University of Helsinki, (Biocenter 1, Viikinkaari 9), Finland

ARTICLE INFO

Edited by: Professor Bing Yan

Keywords:
Textile dyes
Decolorization
White rot fungus *Phanerochaete velutina*
Bioremediation
Nickel and Cobalt salts

ABSTRACT

Organic aromatic compounds used for dyeing and coloring in the textile industry are persistent and hazardous pollutants that must be treated before they are discharged into rivers and surface waters. Therefore, we investigated the potential of the white rot fungus *Phanerochaete velutina* to decolorize commonly used reactive dyes. The fungus decolorized in average 55% of Reactive Orange 16 (RO-16) after 14 days at a maximum rate of 0.09 d^{-1} and a half-life of 8 days. Furthermore, we determined the inhibitory effects of co-present inorganic contaminants Nickel (Ni) and Cobalt (Co) salts on the decolorization potential and determined IC_{50} values of 5.55 mg l^{-1} for Co and a weaker inhibition by Ni starting from a concentration of 20 mg l^{-1}. In the decolorization assay for Remazol Brilliant Blue R (RBBR) we observed the interference of a metabolite of *P. velutina*, which did not allow us to investigate the kinetics of the reaction. The formation of the metabolite, however, could be used to obtain IC_{50} values of 3.37 mg l^{-1} for Co and 7.58 mg l^{-1} for Ni. Our results show that living white rot fungi, such as *P. velutina,* can be used for remediation of dye polluted wastewater, alternatively to enzyme mixtures, even in the co-presence of heavy metals.

1. Introduction

Large quantities of reactive dyes, which are widely used in the textile industry, must be disposed of properly. The dyes are water-soluble, persistent, and can reach concentrations of 10–7000 mg l^{-1} in the effluent wastewater (Saini, 2017; Yaseen and Scholz, 2019). Hazards arise, on the one hand, from mutagenic, carcinogenic, and toxic properties of the dyes (Bayramoglu et al., 2019; Chung, 2016; Leme et al., 2015), and, on the other hand, from their light-absorbing properties that inhibit photosynthesis of plants and lower the level of dissolved oxygen. This lack of oxygen is particularly problematic in textile wastewater effluents that have a large biological oxygen demand (BOD) and a large chemical oxygen demand (COD) (Yaseen and Scholz, 2016). Therefore, the main strategy for treating dye polluted effluent wastewater is the decolorization of the textile dyes. Different techniques based on physical, chemical, and biological approaches have been applied for wastewater treatment of the textile industry, leading to the conclusion that only the combination of different wastewater treatment processes leads to the decomposition and decolorization of commonly used dyes (Hassan and Carr, 2018; Peralta-Zamora et al., 2003). Advancements in the field of biological treatments have been made by exploring fungi species that are known to excrete enzymes capable to degrade highly persistent materials, such as lignin, a class of natural polymers that are also composed of aromatic structures in form of cross-linked phenolic structures (Ponnusamy et al., 2019; Quintella et al., 2019; Singh and Dwivedi, 2020). Potent organisms excrete azoreductases, laccases, lignin peroxidase, and manganese peroxidase (Dauda and Erkurt, 2020; Imran et al., 2014). *Basidiomycetous* represents such an organism that is known to produce nonspecific extracellular oxidoreductive enzymes, which can degrade lignin and xenobiotic compounds (Hatakka et al., 2011).

However, the potential of microorganisms to depollute contaminated wastewater and soils (Sigh et al., 2018; Yin et al., 2019, 2016) is often diminished by co-pollutions of heavy metal ions, such as co-pollutants

* Corresponding author at: University of Natural Resources and Life Sciences, Vienna, Department of Water-Atmosphere-Environment, Institute of Waste Management, Muthgasse 107, 1190 Vienna, Austria.
E-mail address: florian.part@boku.ac.at (F. Part).

https://doi.org/10.1016/j.ecoenv.2021.112093
Received 22 December 2020; Received in revised form 18 February 2021; Accepted 21 February 2021
Available online 12 March 2021

are Nickel (Cempel and Nikel, 2006) and Cobalt (Farjana et al., 2019) ions. In cases of fungi, metal ions inhibited the mycelial growth (Falih, 1997; Hatvani and Mecs, 2003; Liaquat et al., 2020; Sanglimsuwan et al., 1993) or inhibit the activity of enzymes excreted by fungi, such as laccases (Ben Younes et al., 2007; Hatvani and Mecs, 2003; Jeon and Lim, 2017; Sadhasivam et al., 2008; Wang et al., 2010) and manganese peroxidase (Hatvani and Mecs, 2003; Zhang et al., 2016). Investigations on decolorization of reactive dyes mainly focused on biotechnological produced laccases from fungi and yielded fast rates (Çifçi et al., 2019; Kües, 2015; Murugesan et al., 2009; Noman et al., 2019). Although such approaches may be highly efficient due to high enzymatic activities, enzymes that are deactivated by metal ions cannot be recovered anymore and are lost which makes such approaches expensive (Gholami-Borujeni et al., 2011; Mugdha and Usha, 2012; Mukherjee et al., 2013). Alternatively, approaches using living organisms proved also to efficiently degrade reactive dyes (Wang et al., 2017; Yin et al., 2019).

Based on the potential to use fungi to depollute contaminated wastewater, we investigated the fungus *P. velutina* for its ability to sustain its viability and biodegradation potential in the presence of heavy metals. We introduced a miniaturized, high-throughput assay to investigate the performance of white rot fungi cultures to decolorize textile dyes in contaminated wastewater and soils.

2. Materials and methods

2.1. Cultivation of Phanerochaete velutina

The fungus *P. velutina* (FBCC 941, old number 244i) was obtained from the Fungal Biotechnology Culture Collection (FBCC) of the Department of Microbiology of the University of Helsinki in Finland. *P. velutina* is commonly known as basidiomycetous white rot fungus. The fungus was pre-grown on malt extract-agar (MEA) plates for seven days at 28 °C. Five plugs (4 mm diameter each) of inoculated MEA were thereafter dissolved in 75 ml of sterilized LN-AS liquid medium (pH = 4.5) with 0.5% (wt./ vol) glucose as a carbon source in two flasks (250 ml each) and shaken at 28 °C for seven days. After this pre-growth phase, both flasks contained well-grown *P. velutina* biomass, which was well observed as a dense biomass in the solution. Both pre-growth phase flasks were combined and mixed with a sterile stirrer. The resulting mixture was well distributed, as observed from the density of the fungus, and was added to the test plates as 20 μl aliquots.

2.2. Decolorization assay

$NiCl_2 \cdot 6\ H_2O$ (Sigma-Aldrich, Germany), $CoCl_2 \cdot 6\ H_2O$ (Sigma-Aldrich, Germany), and NaCl (Merck, Germany) were dissolved in stocks of low nitrogen-asparagine-succinate (LN-AS solutions, *p*H = 4.5 (Hatakka and Uusi-Rauva, 1983; Moilanen et al., 1996), with 0.5% (wt./ vol) glucose as carbon source. The sterile stock solutions containing either $NiCl_2 \cdot 6\ H_2O$ (Sigma-Aldrich, Germany), $CoCl_2 \cdot 6\ H_2O$ (Sigma-Aldrich, Germany), or NaCl (Merck, Germany) were added to the wells of a 48-wells microtiter plate to yield final concentrations of 0, 50, 100, 500, 1000, 2500, 5000, 7500, 10,000 and 20,000 μg l^{-1} of $NiCl_2$, $CoCl_2$ or NaCl. To these media, 20 μl of autoclaved dye solution, either Reactive Orange 16 (Sigma-Aldrich, Germany, CAS no. 12225-83-1) referred to as 'RO-16' and Remazol Brilliant Blue R (Sigma-Aldrich, Germany, CAS no. 2580-78-1) referred to as 'RBBR', was added to reach a final concentration of 100 mg l^{-1}. A dye concentration of 100 mg l^{-1} was chosen because it represents a realistic concentration of textile dyes found in wastewater from the textile industry (Imran et al., 2014) and exhibited optimal absorbance properties that were useful for the plate reader. Finally, 20 μl of *P. velutina* liquid culture were added to the wells to a final volume of 500 μl per well. Comparative samples were prepared in the wells without the fungus and/or the dye, whereby the corresponding amount of ultrapure water (20 μl or 40 μl, respectively) was added to reach the final volume. All experiments were performed in quadruplicates. In total, six 48 well plates were prepared, using three different salt solutions i.e. NaCl, $CoCl_2$, and $NiCl_2$, and two dyes. A general plate layout displaying the experimental setup is shown in Supplemental Fig. S1. The plates were incubated at 20 °C during the observation period of 14 days. The plates were covered with a lid to avoid contaminations and to keep them sterile. The decolorization efficiency of the fungus was measured as a change of the absorbance in each well using a Tecan Infinite 200 plate reader (Tecan, Austria), which was adjusted to an optimized wavelength for each dye. The absorbance of RO-16 was measured at 504 nm and that of RBBR at 492 nm. The absorbance was measured immediately after the plate was prepared (day 0), as well as at days 3, 6, and 14 (Supplemental Fig. S1). The obtained results were compared to the samples without fungi, where a decay of absorbance at the characteristic wavelengths of the respective dye would indicate oxidative degradation effects. The rate constant k (Supplemental Equation 1) and half-life $\tau_{1/2}$ (Supplemental Equation 2) were determined from transient absorption data using integrated rate laws for first-order reactions.

2.3. Statistical analysis

The analysis for the determination of the statistical significance of the data was performed in Sigma Plot 14.0.3 (Systat Software GmbH, Germany) using two-way ANOVA with *post-hoc* Bonferroni test. A level of $p < 0.05$ was regarded as significant. Dose-response plots for the determination of IC_{50} values were fitted by four parametric logistic curves (Equation 1), also in Sigma Plot.

$$A = A_{min} + \frac{A_{max} - A_{min}}{1 + 10^{\log(EC_{50} - c)k_{Hill}}} \quad (1)$$

Eq. (1). Hill's type four parametric logistic curve with absorption (A), minimum absorption (A_{min}), maximum absorption (A_{max}), the IC_{50} value (EC_{50}), the concentration of the metal salt (c), and the Hillslope (k_{Hill}).

3. Results and discussion

3.1. Oxidative and enzymatic degradation of RO-16

The ability and performance of the white rot fungus *P. velutina* to decolorize the reactive dyes RO-16 and RBBR were investigated for different NaCl concentrations. NaCl was used as the reference substance because it is known to be non-toxic in the concentration range used in this study. This approach enabled to obtain the decolorization rates of the dyes in the absence of inhibitory effects. Fig. 1A shows the time-dependent degradation and decolorization of the dye RO-16 by *P. velutina* where we observed a clear decay of the absorbance signals of the dye in all samples after an incubation of 6 days. This decay became significant for all concentrations after 14 days. The control experiment shown in Fig. 1B, which contained the dye in the buffer solution without *P. velutina*, showed only a small signal decay over all regarded time points in comparison to the situation when the fungus was present (Fig. 1A). This comparison indicated an enzymatic degradation of the dye by the fungus as a function of time, as no significant differences could be observed in the case of the control experiments (Fig. 1B). When comparing all *P. velutina* containing samples (Fig. 1A) it becomes apparent that the degree of decolorization was independent of the concentration of NaCl, which was also statistically confirmed by an ANOVA with post-hoc Bonferroni test. The ANOVA reveals that the relations of incubation time, as well as the concentration, were significant, but not the interaction between these parameters, which indicates, that the degradation was independent at a given time point for a concentration and vice versa (Supplemental Table S1). The *post-hoc* test reveals that for a given time point the concentrations differed significantly in comparison to the control without *P. velutina* and that at a given concentration all combinations of the time points differed among each

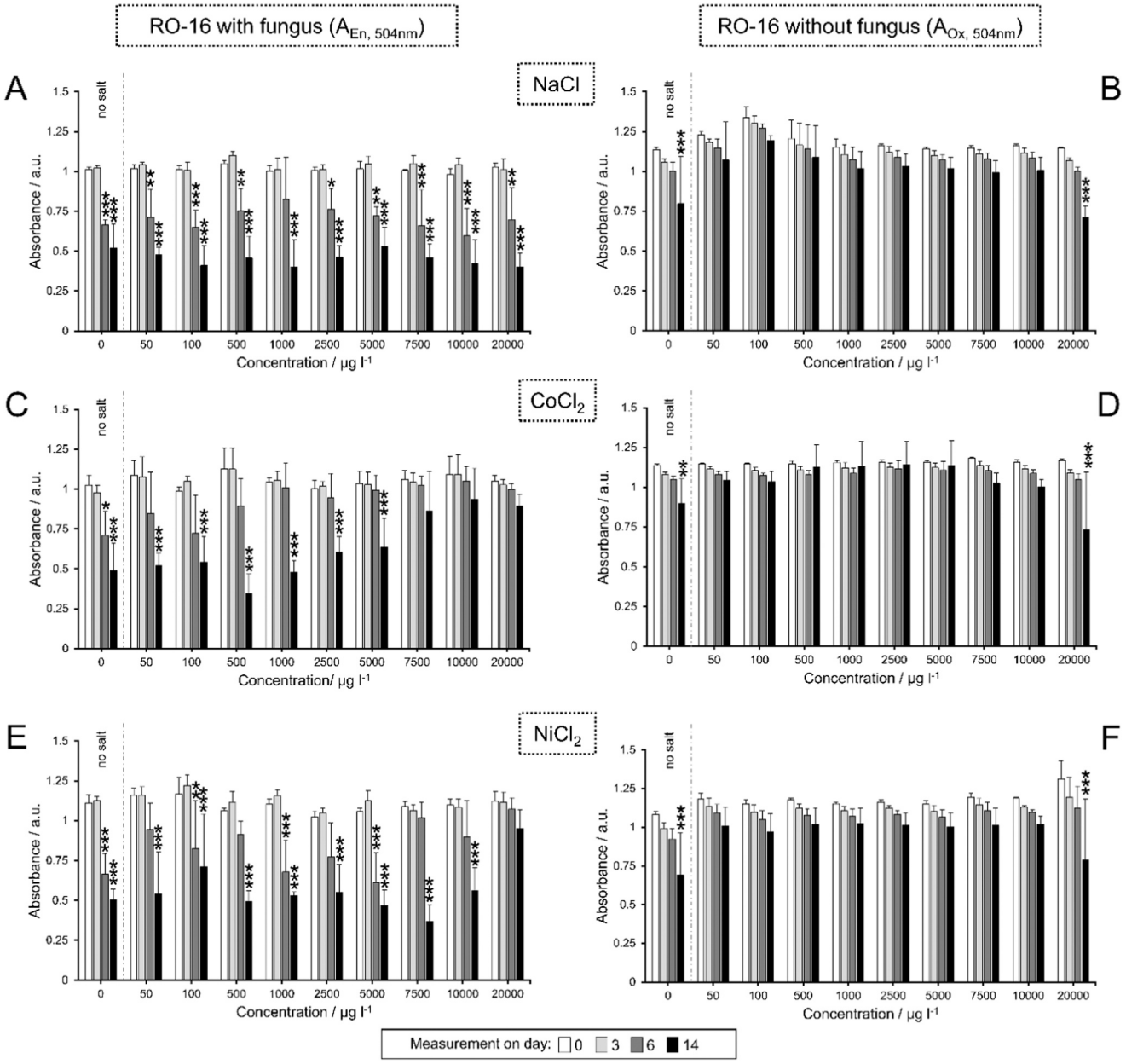

Fig. 1. The decolorization assays show the concentration-dependent absorbance signals at 504 nm of RO-16 dye incubated with *P. velutina* at different concentrations of NaCl (A), $CoCl_2$ (C), and $NiCl_2$ (E). The control experiments of RO-16 without the fungus are shown in B) for NaCl, D) for $CoCl_2$, and F) for $NiCl_2$. The concentration '0' in A, C, and E contained *P. velutina* and no additional salts, while the concentration '0' in B, D, and F did not contain *P. velutina*. The error bars represent the standard deviation of quadruplicate samples. The significance was tested by two-way ANOVA with post-hoc Bonferroni pairwise test using the parameters time point and concentration. The significance is only indicated for day 3, 6, and 14 compared to day 0 with: * for $p < 0.05$, ** for $p < 0.01$, and *** for $p < 0.001$.

other, with exception of day 3 versus 0. Therefore, the results showed that the degradation of RO-16 by *P. velutina* was neither inhibited nor stimulated by any applied concentration within 50–20,000 µg l^{-1} of NaCl and confirms the initial hypothesis that NaCl can be used as a reference substance in this experimental setup. The control experiment (Fig. 1B) shows that also in the absence of the fungus, small amounts of RO-16 were degraded with time at almost all concentrations of NaCl, which suggested that the dye was oxidized. A similar ANOVA, as conducted for the experiment containing *P. velutina*, revealed that some signal decays were statistically significant, particularly towards day 14, but only for the highest concentration (20,000 µg l^{-1}), suggesting that the oxidation of RO-16 is favored at higher salinity (Supplemental Table S1). However, the extent of oxidation processes was lower than that of the enzymatic degradation, which was also evaluated by ANOVA, comparing the absorbance data for each day and each concentration, that confirmed a significant higher degradation in the presence of *P. velutina* for almost all concentrations at all time points (Supplemental Table S4).

The extent of the enzymatic degradation compared to the oxidation of RO-16 is shown in Fig. 2A in form of relative values (given as A_{Ox} / A_{En} −1). This representation plots the extent of the enzymatic degradation as positive values, while negative values indicate dominant oxidation of the dye. The results for NaCl show that the enzymatic degradation led first to increased RO-16 degradation of 11–26% on day 0 compared to the pure oxidation. Until day 3 the enzymatic activity decreased to 5–24% and increased again to 25–55% on day 6 and 43–80% on day 14. Thus, the initial assumption that NaCl is not inhibitory at the concentrations used was confirmed.

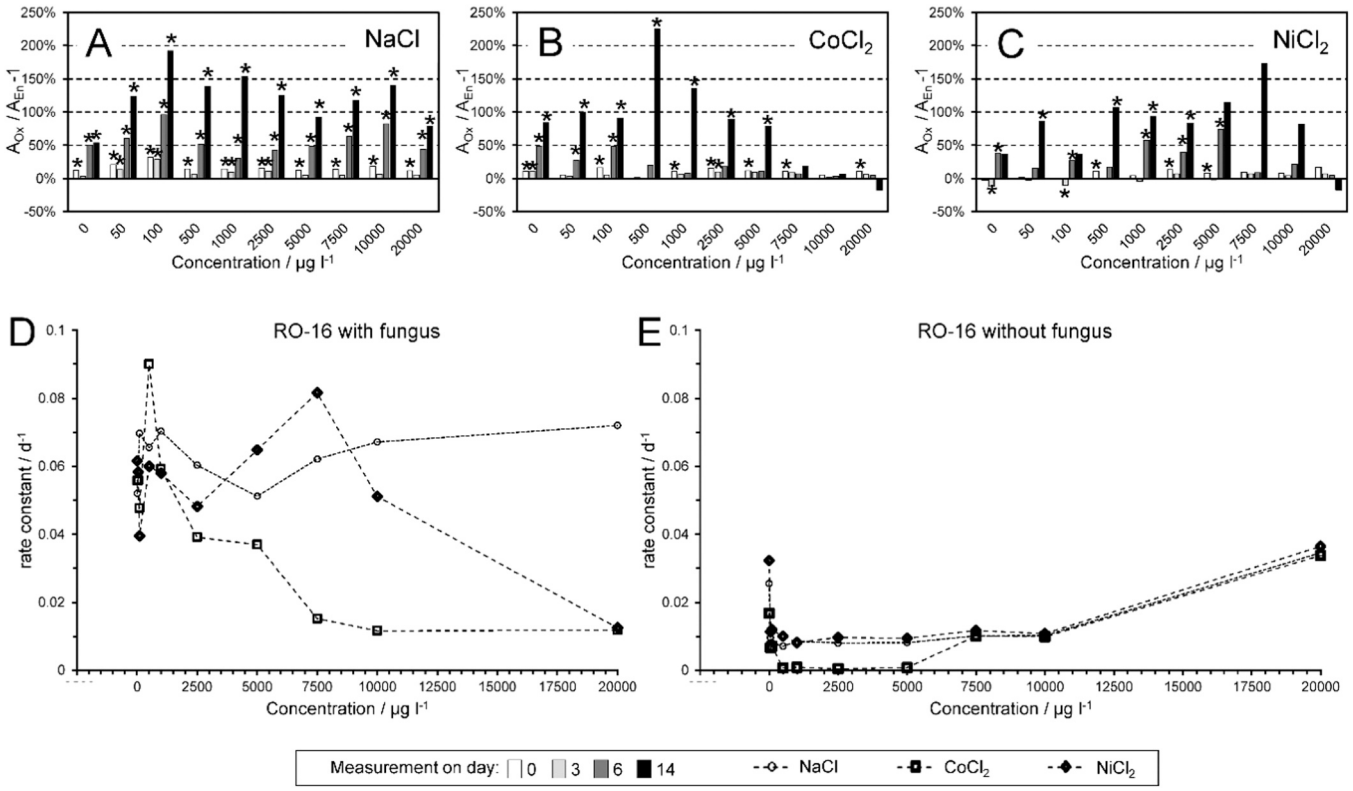

Fig. 2. The barcharts show the relative extents of the degradation of RO-16 from absorbance data with *P. velutina* (A_{En}) indicating an enzymatic degradation and without the fungus (A_{Ox}) indicating the oxidation. Positive values indicate a dominant enzymatic reaction and negative values a dominant oxidation reaction. A) for NaCl, B) for $CoCl_2$, and C) for $NiCl_2$. Rate constants that were based on first order kinetics are shown in D) for fungus containing samples (enzymatic degradation) and E) for samples without *P. velutina* (oxidation). Significances in A, B, and C were obtained from two-way ANOVA comparing data with and without *P. velutina* for different concentrations and on different days, with * for $p < 0.05$.

When $CoCl_2$ was co-exposed with RO-16 and *P. velutina* (Fig. 1C) we observed also decays of the absorbance, but also the formation of a minimum that is most pronounced at a concentration of 500 µg l^{-1} on day 14. This minimum indicated the maximal degradation of RO-16. We find significant differences in the signal decrease on day 14 for concentration < 7500 µg l^{-1}, which means concentrations > 5000 µg l^{-1} of $CoCl_2$ acted inhibitory on the degradation of RO-16 (Supplemental Table S2). However, the same analysis showed that these differences became only significant for day 14. The control experiment without *P. velutina* (Fig. 1D) showed no apparent features, except for small and significant decays on day 14 at 0 and 20,000 µg l^{-1} of $CoCl_2$ (Supplemental Table S2). This finding indicates that the oxidation of RO-16 was inhibited when $CoCl_2$ was added in a range of 50–10,000 µg l^{-1}. When we compared the samples with and without the fungus for each time point (Fig. 1C and D), we found that the absorbance was significantly lower when no $CoCl_2$ was present and decays became significant towards day 14 for concentrations up to 5000 µg l^{-1} (Supplemental Table S2). Interestingly, we found significant differences at most concentrations on day 0 (except for 50, 500 and 10,000 µg l^{-1}) that vanished on day 3 and became significant towards day 6 and 14 (Fig. 2B). Moreover, the results showed that the enzymatic degradation was dominating, particularly on day 14 and for concentrations up to 5000 µg l^{-1}, while at higher concentrations of $CoCl_2$ no differences to the oxidation reaction were observed.

The influence of $NiCl_2$ on the degradation of RO-16 by *P. velutina* is shown in Fig. 1E, where we found significant degradations on day 14 for all concentrations except of 20,000 µg l^{-1} (Supplemental Table S3). In the absence of the fungus (Fig. 1F), we found differences only for 0 and 20,000 µg l^{-1} on day 14, which indicated a weak oxidation. In comparison to the oxidation, the enzymatic degradation was most pronounced by up to 70%, on day 14 at 7500 µg l^{-1}. Overall, $NiCl_2$ showed inhibiting effects on day 6 for concentrations > 5000 and on day 14 for concentrations > 7500 µg l^{-1} (Fig. 2C). This finding suggested that *P. velutina* was inhibited in its enzymatic activity and recovered after day 6.

For a comparison of oxidative and enzymatic degradation we calculated rate constants assuming first order kinetics based on the absorbance data (Fig. 2). The calculations showed that in case of NaCl the rate of degradation was increasing with increasing salt concentration and became constant at ca. 0.065 d^{-1} for concentrations ≥ 2500 µg l^{-1} (Supplemental Tables S7 and S8). For $CoCl_2$ we found a maximum of the rate at 500 µg l^{-1} (0.09 d^{-1}) that declined to a minimum of ca. 0.01 d^{-1} for concentrations ≥ 7500 µg l^{-1}. $NiCl_2$ exhibited a maximum rate of 0.081 d^{-1} at 7500 µg l^{-1} and decreased later to 0.01 d^{-1} for the highest concentration. These observations were similar to those of Murugesan et al. (2009), who also showed that during decolorization by fungal enzymes, the inhibitory effect of co-exposed Ni salts was weaker than that of Co at concentrations > 5 mM. Without *P. velutina*, when only oxidative degradation was possible, we found decreasing degradation rates in all cases (Fig. 2E) that remained at ca. 0.01 d^{-1} for Na and Ni in a range of 50–10,000 µg l^{-1}, while we found a characteristic minimum with a 10-fold lower rate in between 500 and 5000 µg l^{-1} in case of Co. This finding suggested that Co inhibited the oxidation stronger than Na and Ni in the same range of concentrations. Interestingly, for concentrations of 10,000 and 20,000 µg l^{-1}, the individual difference of the metals vanished and yielded similar rates.

3.2. Oxidative and enzymatic degradation of RBBR

The degradation of RBBR was remarkably different from our findings found for RO-16. For NaCl (Fig. 3A) we found no significant decrease in absorbance and thus it appeared that RBBR was not enzymatically

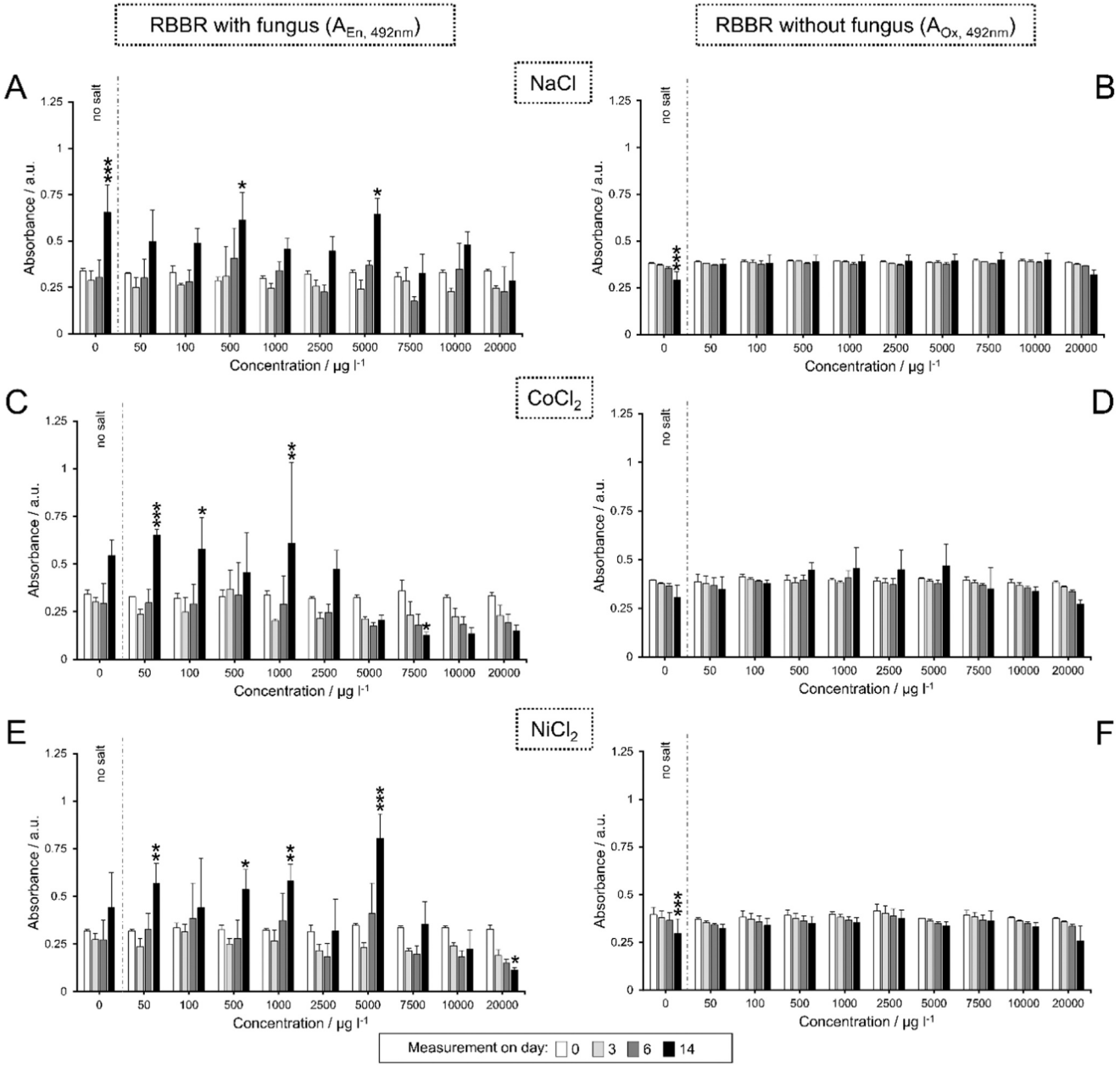

Fig. 3. The decolorization assays show the concentration-dependent absorbance signals at 492 nm of RO-16 dye incubated with *P. velutina* at different concentrations of NaCl (A), $CoCl_2$ (C), and $NiCl_2$ (E). The control experiments of RO-16 without the fungus are shown in B) for NaCl, D) for $CoCl_2$, and F) for $NiCl_2$. The concentration '0' in A, C, and E contained *P. velutina* and no additional salts, while the concentration '0' in B, D, and F did not contain *P. velutina*. The error bars represent the standard deviation of quadruplicate samples. The significance was tested by two-way ANOVA with post-hoc Bonferroni pairwise test using the parameters time point and concentration. The significance is only indicated for day 3, 6, and 14 compared to day 0 with: * for $p < 0.05$, ** for $p < 0.01$, and *** for $p < 0.001$.

degraded at any concentration. Moreover, an increase of absorbance compared to the initial level on day 0 was found on day 14 for all concentrations, with exception of 7500–20,000 µg l^{-1}. The absorption exhibited strong variations that were statistically significant only at concentrations of 500–5000 µg l^{-1} (Supplement Table S9 and S12). The control experiment without the fungus (Fig. 3B) showed stable signals and a lack of significant oxidative degradation, with exception of concentrations 0 and 20,000 µg l^{-1} on day 14. The surprising increase in absorbance in the presence of *P. velutina*, whereas no increase was detected in the absence of the fungus, indicated that the increasing absorbance originated from a metabolite that interferes at the same wavelength as RBBR (492 nm).

When $CoCl_2$ was exposed to *P. velutina*, we found an increase of absorbance up to a concentration of 2500 µg l^{-1} (Fig. 3C), while all concentrations above 2500 µg l^{-1} showed decreasing absorptions over time, which suggests that RBBR was decolorized (statistical data are given in Supplement Table S10 and S13). At the threshold concentration of 2500 µg l^{-1} of $CoCl_2$, we found also the inhibition of the RO-16 degradation (cf. Fig. 1C), which suggested that this threshold would also apply for RBBR. These findings, in turn, confirm that an increase of absorbance reflected the non-inhibited enzymatic activity of *P. velutina*. The oxidative degradation of RBBR in the presence of $CoCl_2$ was minimal and not significant. (Fig. 3D).

In the case of $NiCl_2$ (Fig. 3E), we found also increasing absorbance signals towards day 14, but with a higher concentration onset at $\geq$ 10,000 µg l^{-1} than in the case of $CoCl_2$. The onset of the signal decrease matched well the highest concentration that still showed significant degradation of RO-16 (cf. Fig. 1E). Therefore, also our findings

for $NiCl_2$ confirmed that the increasing adsorption of the unknown compound was connected to the metabolism of *P. velutina* (statistical data are given in the Supplement table S11 and S14). The oxidation of RBBR was also low in the presence of $NiCl_2$ with exceptions at 0 and 20,000 μg l^{-1} (Fig. 3F).

For all investigated salts, RBBR showed increasing absorbance signals in the presence of *P. velutina* (Fig. 3A, C, and E) at 492 nm, from day 6–14, for the same concentrations that were found to be not inhibitory for the fungus when degrading RO-16, which suggested that this increase in absorbance was caused by a metabolite of the fungus. Also, the trend of the absorbance data from day 0–6 indicated a reduced absorbance for non-inhibitory concentration in experiments with *P. velutina* and RO-16, which suggested that RBBR was degraded at these early time points. However, based on the available data it remains elusive if the metabolite, putatively responsible for the later increasing absorbance, was associated with a metabolite of RBBR, or *P. velutina* formed the compound independently of the dye. We consider the formation of an RBBR independent metabolite as the most reasonable case, based on the finding that the absorbance was initially decreasing and that the absorbance on day 14 was exceeding the initial absorbance. This exceeding absorbance suggested that the newly formed metabolite exhibited an absorptivity larger than RBBR at 492 nm. The reason for not observing the metabolite in the experiments with RO-16 might have originated from its weak absorptivity at 504 nm.

Like RO-16, we calculated relative absorbance data with and without *P. velutina* to understand which reaction, enzymatic or oxidative, was dominant and to what extent compared to the other (Fig. 4). In contrast to the data that we obtained for RO-16, we found almost exclusive negative values for day 14 in NaCl, which were not caused by an oxidative reaction, but by the already described increase in absorption caused by the unknown metabolite. Therefore, these data represent a sum parameter of the oxidative degradation and the formation of the unknown metabolite. This increase in absorption was up to 50% compared to the samples without *P. velutina* (Fig. 4A).

For $CoCl_2$ we found that the enzymatic degradation of RBBR was dominating at all concentrations with exception of concentrations from 0 at 2500 μg l^{-1} for day 14, which was caused again by the absorbance increase of the unknown metabolite (Fig. 4B). Interestingly, the ratio (A_{Ox} / A_{En} −1) shows that the onset of the metabolite generation on day 14 was inhibited linearly in a concentration range from 0 to 2500 μg l^{-1} $CoCl_2$, that changed to a steep inhibition in between 2500 and 5000 μg l^{-1}, where the enzymatic degradation was dominating and raised from ca. 0–150% (Fig. 4B, black bars). For days 0–6, we found exclusively enzymatic degradation.

For $NiCl_2$ we found a similar behavior as for $CoCl_2$, indicated by a shift of the enzymatic degradation for concentration $>$ 7500 μg l^{-1} on day 14 (Fig. 4C). From day 0–6 the only the enzymatic degradation was dominant. The unknown metabolite interfered also with our calculation of rate constants which was made for RBBR based on the same kinetic model as for RO-16. As expected from the data the increasing absorbance resulted in negative rate constants (Fig. 4D). This was the case for NaCl with exception of a concentration of 20,000 μg l^{-1}, which had a low coefficient of determination R^2 (Supplement Table S14). For $CoCl_2$ we obtained reasonable rates, according to R^2, for concentrations $\geq$ 7500 μg l^{-1} ranging from 0.07 to 0.053 d^{-1}, which corresponds to a half-life of 10–13 days. In the case of $NiCl_2$, only the highest concentration was reasonable and resulted in a rate constant of 0.068 d^{-1} at a concentration of 20,000 μg l^{-1} and a half-life of 10.2 days. For the oxidative degradation (Fig. 4E), we obtained in almost all cases and concentrations used reasonable R^2 values (Supplement Table S15). Like RO-16 (cf. Fig. 4E), the oxidative degradation of RBBR exhibited the highest rates at the lowest and the highest concentration of 0 and

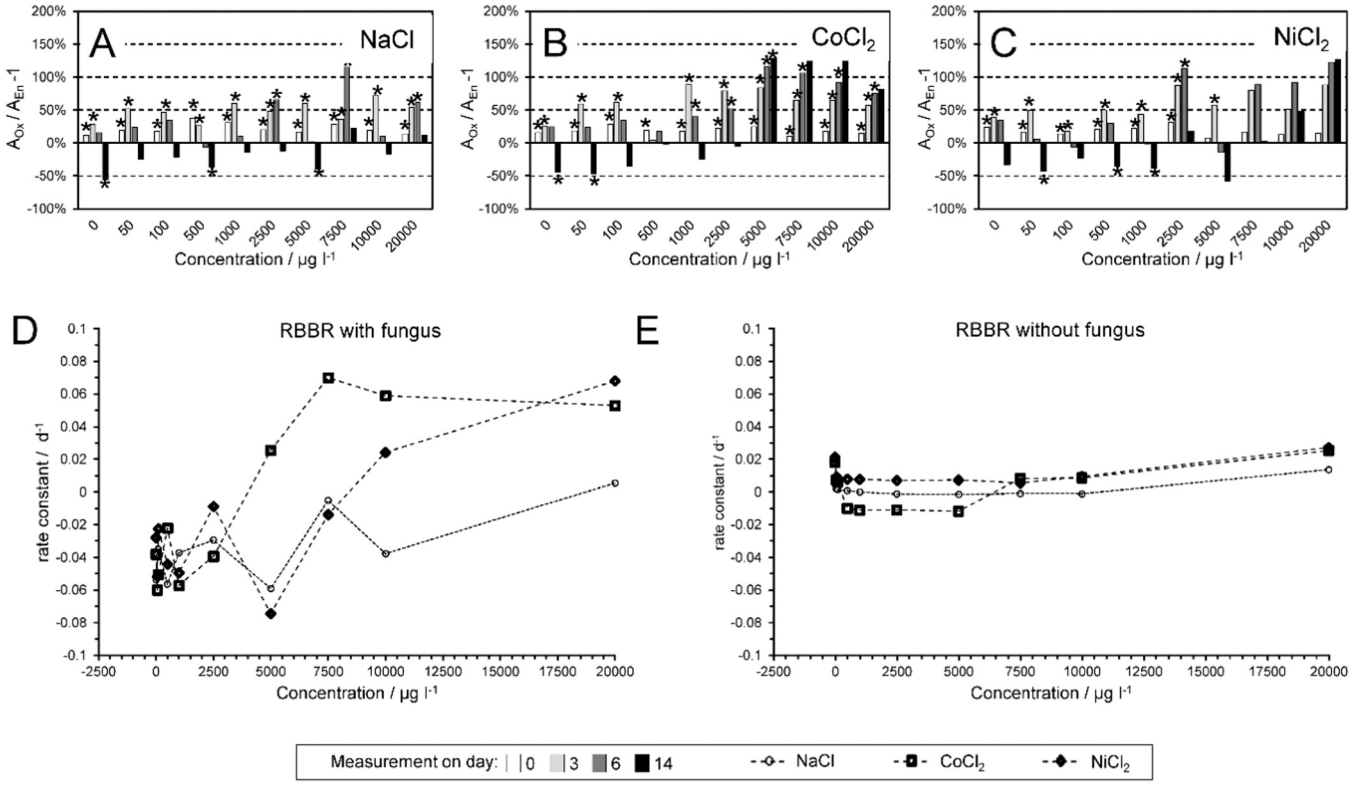

Fig. 4. The bar charts show the relative extent of the degradation of RO-16 from absorbance data with *P. velutina* (A_{En}) indicating an enzymatic degradation and without the fungus (A_{Ox}) indicating the oxidation. Positive values indicate a dominant enzymatic reaction and negative values a dominant oxidation reaction. A) for NaCl, B) for $CoCl_2$, and C) for $NiCl_2$. Rate constants that were based on first-order kinetics are shown in D) for fungus containing samples (enzymatic degradation) and E) for samples without *P. velutina* (oxidation). Significances in A, B, and C were obtained from two-way ANOVA comparing data with and without *P. velutina* for different concentrations and on different days, with * for $p < 0.05$.

20,000 μg l^{-1}. The rates for the oxidative oxidation ranged from 0.014 to 0.027 d^{-1} with half-lives of 25–50 d.

3.3. Metal dose-response on decolorization

Dose-response curves for the degradation were calculated by 4 parametric logistic curves based on Hill's equation and considering quadruplicate measurements for all days. For the early time points (0, 3, and 6 days), we could not find reasonable sigmoidal fits for both dyes (Supplement Fig. S2 and S3 with data on fits in Table S17–S22). In the case of RO-16, a reasonable sigmoidal fit with an inhibitory concentration (IC_{50}) of 5.55 mg l^{-1} (Fig. 5B, Table 1) could only be determined for $CoCl_2$, which was already expectable from the absorbance data, since only on day 14 a concentration dependency could be observed (c.f. Fig. 1). In the case of $NiCl_2$, only the highest concentration was inhibitory on day 14 (Fig. 5C), which was too less to fit a dose-response curve, while NaCl did not inhibit the decolorization in the applied concentration range and return a flat dose-response curve (Fig. 5A).

Sigmoidal type curves were also obtained for RBBR on day 14 for $CoCl_2$ and $NiCl_2$ (Fig. 5E and F), however, the shape of these curves was inverse to the case of RO-16. This inverse shape of the curves was attributed to the formation of the unknown metabolite and its inhibition at higher concentrations of $CoCl_2$ and $NiCl_2$ described earlier in this work. IC_{50} calculations yielded 3.37 mg l^{-1} for $CoCl_2$ and 7.58 mg l^{-1} for $NiCl_2$ (Table 1), which suggested that $CoCl_2$ had a stronger inhibitory effect on the metabolism of the *P. velutina* than $NiCl_2$. This finding was similar to the behavior found for the fungus *Ganoderma lucidum* described in the literature (Zhang et al., 2016).

A comparison of the IC_{50} data from our study with toxicity data from the literature for 21 fungi species shows that decolorization is more sensitive than the minimal inhibitory concentration (MIC) by cell counting (Sanglimsuwan et al., 1993). The MIC was obtained after 7 days of incubation and yielded 1–5 mM for Co and 0.7–7 mM for Ni, while we obtained 0.014 and 0.023 mM (3.37 and 5.55 mg l^{-1}) for Co and 0.032 mM (7.58 mg l^{-1}) for Ni after 14 days. This comparison also suggested that the inhibitory effects found in our study originate from an extracellular deactivation of the excreted enzymes responsible for decolorization of the dyes, rather than a toxic effect on the fungi. In turn, the IC_{50} of Ni and Co for *P. velutina* is much higher than concentrations typically found in wastewaters from the textile industry ranging from 0.070–1.56 mg l^{-1} for Ni and 0.02–0.06 mg l^{-1} for Co (Hussein, 2013; Imtiazuddin et al., 2012; Joshi and Santani, 2012; Manekar et al., 2014). This comparison indicated that *P. velutina* – and possibly other related white rot fungi species – is resilient to inhibition and toxic effects in wastewater effluents from the textile industry and is thus a suitable candidate for decolorization and remediation purposes.

4. Conclusions

The present study shows that a search of potent organisms for bioremediation of textile dye polluted wastewater can be made by miniaturized high-throughput decolorization assays. This approach enables the assessment of the performance of microorganisms to decolorize textile dyes and the resilience towards co-pollutants, such as heavy metals at realistic concentrations. However, metabolites formed by the microorganisms can interfere with the optical properties of the dyes, which restrict the usability of such assays. For our model organism, the white rot fungus *P. velutina*, we found a clear ability to decolorize known persistent reactive dyes RO-16. The fungus proved to be resilient to Ni and Co at concentrations typical for wastewaters from the textile industry, which qualifies this organism for bioremediatory applications.

CRediT authorship contribution statement

Christian Zafiu: Conceptualization, Methodology, Formal analysis, Writing - original draft, Visualization. **Florian Part**: Conceptualization, Methodology, Project administration, Writing - review & editing. **Eva-Kathrin Ehmoser**: Writing - review & editing. **Mika A. Kähkönen**: Conceptualization, Methodology, Investigation, Resources, Writing - original draft, Supervision, Funding acquisition.

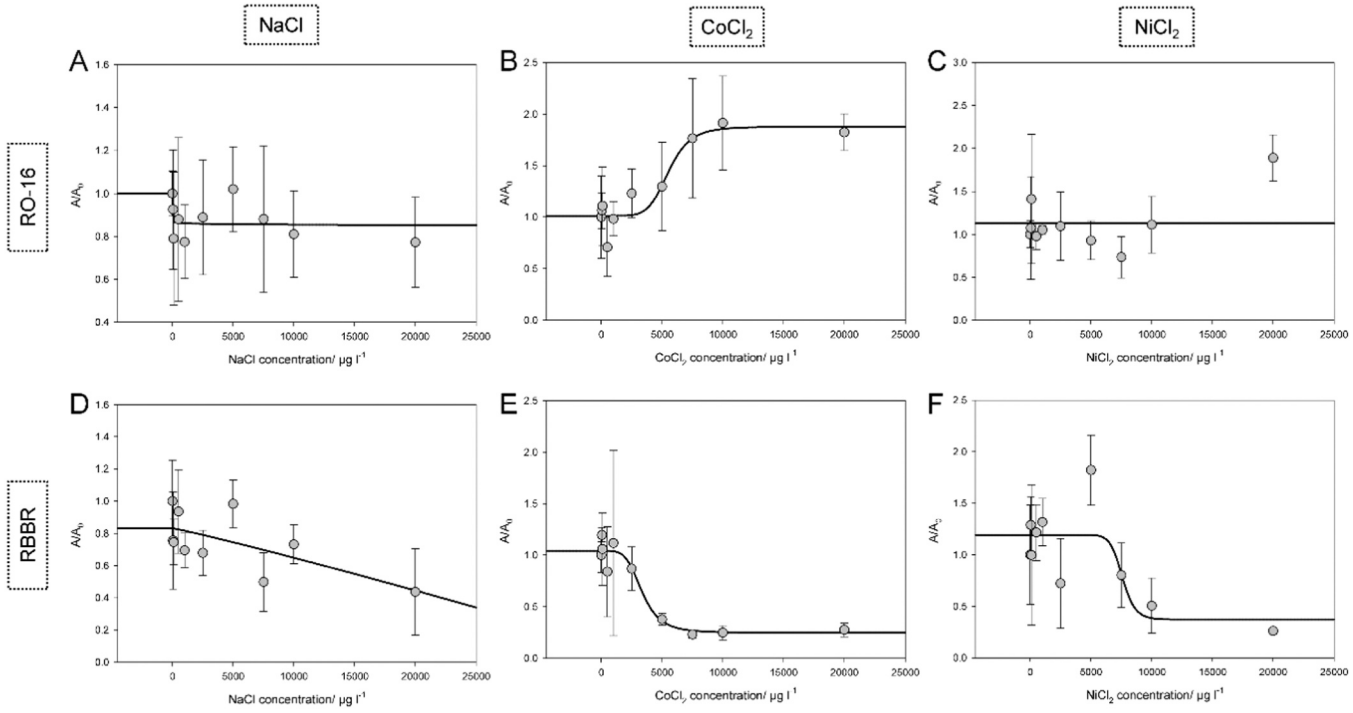

Fig. 5. Upper panels: Dose-response curves fitted by 4 parametric logistic curves based on Hill equation for RO-16 on day 14 spiked with NaCl (A), $CoCl_2$ (B), and $NiCl_2$. (C). Lower panels: Dose-response curves for RBBR spiked with NaCl (D), $CoCl_2$ (E), and $NiCl_2$ (F). Absorbance was normalized by the corresponding control "0" sample without dyes. The reference absorbance A_0 is the mean value of concentration 0 at the respective time point.

Table 1
IC_{50} (μg l^{-1}) values and p-values from dose-response curves fit by 4 parametric logistic curves (Hill equation).

Treatment	day	0	3	6	14
Reactive Orange 16					
NaCl	IC_{50} / μg l^{-1}	603.1	62,677.0	73.6	2,638,480.6
	P value	1	1	1	1
$CoCl_2$	IC_{50} / μg l^{-1}	1	41.7	495.8	5546.7
	P value	1	1	1	< 0.0001
$NiCl_2$	IC_{50} / μg l^{-1}	1	1161.8	0.0	80.8
	P value	1	1	1	1
Remazol Brilliant Blue R					
NaCl	IC_{50} / μg l^{-1}	63.1	631.9	17,365,629	15,642,281
	P value	0.3736	1	0.9999	0.9998
$CoCl_2$	IC_{50} / μg l^{-1}	214,296.3	670.6	2509.6	3365.4
	P value	1	1	0.9998	0.0007
$NiCl_2$	IC_{50} / μg l^{-1}	7224.5	0.0	0.0	7581.3
	P value	0.8409	1	1	< 0.0001

Declaration of Competing Interest

The authors declare that they have no known competing financial interests or personal relationships that could have appeared to influence the work reported in this paper.

Acknowledgments

The authors acknowledge the financial support of the Maj and Tor Nessling Foundation in Finland. We also acknowledge Dr. Donatella Tesei, University of Natural Resources and Life Sciences Vienna, Institute of Microbiology and Microbial Biotechnology, for proofreading the manuscript.

Appendix A. Supporting information

Supplementary data associated with this article can be found in the online version at doi:10.1016/j.ecoenv.2021.112093.

References

Bayramoglu, G., Salih, B., Akbulut, A., Arica, M.Y., 2019. Biodegradation of cibacron blue 3GA by insolubilized laccase and identification of enzymatic byproduct using MALDI-ToF-MS: toxicity assessment studies by daphnia magna and chlorella vulgaris. Ecotoxicol. Environ. Saf. https://doi.org/10.1016/j.ecoenv.2018.12.014.

Ben Younes, S., Mechichi, T., Sayadi, S., 2007. Purification and characterization of the laccase secreted by the white rot fungus perenniporia tephropora and its role in the decolourization of synthetic dyes. J. Appl. Microbiol. 102, 1033–1042. https://doi.org/10.1111/j.1365-2672.2006.03152.x.

Cempel, M., Nikel, G., 2006. Nickel: a review of its sources and environmental toxicology. Pol. J. Environ. Stud. 15, 375–382.

Chung, K.T., 2016. Azo dyes and human health: a review. J. Environ. Sci. Health Part C Environ. Carcinog. Ecotoxicol. Rev. https://doi.org/10.1080/10590501.2016.1236602.

Çifçi, D.I., Atav, R., Güneş, Y., Güneş, E., 2019. Determination of the color removal efficiency of laccase enzyme depending on dye class and chromophore. Water Sci. Technol. 80, 134–143. https://doi.org/10.2166/wst.2019.255.

Dauda, M.Y., Erkurt, E.A., 2020. Investigation of reactive blue 19 biodegradation and byproducts toxicity assessment using crude laccase extract from trametes versicolor. J. Hazard. Mater. https://doi.org/10.1016/j.jhazmat.2019.121555.

Falih, A.M., 1997. Influence of heavy-metals toxicity on the growth of phanerochaete chrysosporium. Bioresour. Technol. 60, 87–90. https://doi.org/10.1016/S0960-8524(96)00177-0.

Farjana, S.H., Huda, N., Mahmud, M.A.P., Lang, C., 2019. Life-cycle assessment of solar integrated mining processes: a sustainable future. J. Clean. Prod. 236 https://doi.org/UNSP 11761010.1016/j.jclepro.2019.117610.

Gholami-Borujeni, F., Mahvi, A.H., Nasseri, S., Faramarzi, M.A., Nabizadeh, R., Alimohammadi, M., 2011. Enzymatic treatment and detoxification of acid orange 7 from textile wastewater. Appl. Biochem. Biotechnol. https://doi.org/10.1007/s12010-011-9345-5.

Hassan, M.M., Carr, C.M., 2018. A critical review on recent advancements of the removal of reactive dyes from dyehouse effluent by ion-exchange adsorbents. Chemosphere. https://doi.org/10.1016/j.chemosphere.2018.06.043.

Hatakka, A., Hammel, K.E., 2011. Fungal biodegradation of lignocelluloses. In: Hofrichter, M. (Ed.), Industrial Applications. Springer-Verlag, Berlin Heidelberg, pp. 319–340.

Hatakka, A., Uusi-Rauva, A.K., 1983. Degradation of 14C-labelled poplar wood lignin by selected white-rot fungi. Eur. J. Appl. Microbiol. Biotechnol. 17, 235–242. https://doi.org/10.1007/BF00510422.

Hatvani, N., Mecs, I., 2003. Effects of certain heavy metals on the growth, dye decolorization, and enzyme activity of lentinula edodes. Ecotoxicol. Environ. Saf. 55, 199–203. https://doi.org/10.1016/S0147-6513(02)00133-1.

Hussein, F.H., 2013. Chemical properties of treated textile dyeing wastewater. Asian J. Chem. 25, 9393–9400.

Imran, M., Crowley, D.E., Khalid, A., Hussain, S., Mumtaz, M.W., Arshad, M., 2014. Microbial biotechnology for decolorization of textile wastewaters. Rev. Environ. Sci. Biotechnol. https://doi.org/10.1007/s11157-014-9344-4.

Imtiazuddin, S.A., Mumtaz, M., Mallick, K.A., 2012. Pollutants of wastewater characteristics in textile industries. J. Basic Appl. Sci. 8, 554–556. https://doi.org/10.6000/1927-5129.2012.08.02.47.

Jeon, S.J., Lim, S.J., 2017. Purification and characterization of the laccase involved in dye decolorization by the white-rot fungus marasmius scorodonius. J. Microbiol. Biotechnol. 27, 1120–1127. https://doi.org/10.4014/jmb.1701.01004.

Joshi, V.J., Santani, D.D., 2012. Physicochemical characterization and heavy metal concentration in effluent of textile industry. Univ. J. Environ. Res. Technol. 2, 93–96.

Kües, U., 2015. Fungal enzymes for environmental management. Curr. Opin. Biotechnol. 33, 268–278. https://doi.org/10.1016/j.copbio.2015.03.006.

Leme, D.M., De Oliveira, G.A.R., Meireles, G., Brito, L.B., Rodrigues, L.D.B., Palma De Oliveira, D., 2015. Eco- and genotoxicological assessments of two reactive textile dyes. J. Toxicol. Environ. Health Part A Curr. Issues. https://doi.org/10.1080/15287394.2014.971208.

Liaquat, F., Munis, M.F.H., Haroon, U., Arif, S., Saqib, S., Zaman, W., Khan, A.R., Shi, J., Che, S., Liu, Q., 2020. Evaluation of metal tolerance of fungal strains isolated from contaminated mining soil of Nanjing, China. Biology 9 (12). https://doi.org/10.3390/biology9120469.

Manekar, P., Patkar, G., Aswale, P., Mahure, M., Nandy, T., 2014. Detoxifying of high strength textile effluent through chemical and bio-oxidation processes. Bioresour. Technol. 157, 44–51.

Moilanen, A.M., Lundell, T., Vares, T., Hatakka, A., 1996. Manganese and malonate are individual regulators for the production of lignin and manganese peroxidase isozymes and in the degradation of lignin by phlebia radiata. Appl. Microbiol. Biotechnol. 45, 792–799. https://doi.org/10.1007/s002530050764.

Mugdha, A., Usha, M., 2012. Enzymatic treatment of wastewater containing dyestuffs using different delivery systems. Sci. Rev. Chem. Commun. 2 (1), 31–40.

Mukherjee, S., Basak, B., Bhunia, B., Dey, A., Mondal, B., 2013. Potential use of polyphenol oxidases (PPO) in the bioremediation of phenolic contaminants containing industrial wastewater. Rev. Environ. Sci. Biotechnol. https://doi.org/10.1007/s11157-012-9302-Y.

Murugesan, K., Kim, Y.M., Jeon, J.R., Chang, Y.S., 2009. Effect of metal ions on reactive dye decolorization by laccase from ganoderma lucidum. J. Hazard. Mater. 168, 523–529.

Noman, E., Al-Gheethi, A., Mohamed, R.M.S.R., Talip, B.A., 2019. Myco-remediation of xenobiotic organic compounds for a sustainable environment: a critical review. Topics in Current Chemistry. Springer International Publishing. https://doi.org/10.1007/s41061-019-0241-8.

Peralta-Zamora, P., Pereira, C.M., Tiburtius, E.R.L., Moraes, S.G., Rosa, M.A., Minussi, R. C., Duran, N., 2003. Decolorization of reactive dyes by immobilized laccase. Appl. Catal. B Environ. 42, 131–144.

Ponnusamy, V.K., Nguyen, D.D., Dharmaraja, J., Shobana, S., Banu, J.R., Saratale, R.G., Chang, S.W., Kumar, G., 2019. A review on lignin structure, pretreatments, fermentation reactions and biorefinery potential. Bioresour. Technol. 271, 462–472. https://doi.org/10.1016/j.biortech.2018.09.070.

Quintella, C.M., Mata, A.M.T., Lima, L.C.P., 2019. Overview of bioremediation with technology assessment and emphasis on fungal bioremediation of oil contaminated soils. J. Environ. Manag. https://doi.org/10.1016/j.jenvman.2019.04.019.

Sadhasivam, S., Savitha, S., Swaminathan, K., Lin, F.H., 2008. Production, purification and characterization of mid-redox potential laccase from a newly isolated trichoderma harzianum WL1. Process Biochem. 43, 736–742. https://doi.org/10.1016/j.procbio.2008.02.017.

Saini, R.D., 2017. Textile dye wastewater characteristics and constituents of synthetic effluents. Int. J. Chem. Eng. Res. 9, 121–136.
Sanglimsuwan, S., Yoshida, N., Morinaga, T., Murooka, Y., 1993. Resistance to and uptake of heavy-metals in mushrooms. J. Ferment. Bioeng. 75, 112–114. https://doi.org/10.1016/0922-338x(93)90220-3.
Sigh, R., Ahirwar, N.K., Tiwari, J., Pathak, J., 2018. Review on sources and effect of heavy metal in soil: its bioremediation. Int. J. Res. Appl., Nat. Soc. Sci. Spec. Ed. 1–22.
Singh, G., Dwivedi, S.K., 2020. Decolorization and degradation of direct blue-1 (Azo dye) by newly isolated fungus aspergillus terreus GS28, from sludge of carpet industry. Environ. Technol. Innov. https://doi.org/10.1016/j.eti.2020.100751.
Wang, N., Chu, Y., Wu, F., Zhao, Z., Xu, X., 2017. Decolorization and degradation of Congo red by a newly isolated white rot fungus, Ceriporia lacerata, from decayed mulberry branches. Int. Biodeterior. Biodegrad. 117, 236–244. https://doi.org/10.1016/j.ibiod.2016.12.015.
Wang, Z.X., Cai, Y.J., Liao, X.R., Tao, G.J., Li, Y.Y., Zhang, F., Zhang, D.B., 2010. Purification and characterization of two thermostable laccases with high cold adapted characteristics from pycnoporus sp SYBC-L1. Process Biochem. 45, 1720–1729. https://doi.org/10.1016/j.procbio.2010.07.011.
Yaseen, D.A., Scholz, M., 2019. Textile dye wastewater characteristics and constituents of synthetic effluents: a critical review. Int. J. Environ. Sci. Technol. https://doi.org/10.1007/s13762-018-2130-z.
Yaseen, D.A., Scholz, M., 2016. Shallow pond systems planted with Lemna minor treating azo dyes. Ecol. Eng. https://doi.org/10.1016/j.ecoleng.2016.05.081.
Yin, K., Lv, M., Wang, Q., Wu, Y., Liao, C., Zhang, W., Chen, L., 2016. Simultaneous bioremediation and biodetection of mercury ion through surface display of carboxylesterase E2 from Pseudomonas aeruginosa PA1. Water Res. https://doi.org/10.1016/j.watres.2016.07.053.
Yin, K., Wang, Q., Lv, M., Chen, L., 2019. Microorganism remediation strategies towards heavy metals. Chem. Eng. J. https://doi.org/10.1016/j.cej.2018.10.226.
Zhang, H., Zhang, S., He, F., Qin, X., Zhang, X.Y., Yang, Y., 2016. Characterization of a manganese peroxidase from white-rot fungus trametes sp.48424 with strong ability of degrading different types of dyes and polycyclic aromatic hydrocarbons. J. Hazard. Mater. 320, 265–277. https://doi.org/10.1016/j.jhazmat.2016.07.065.